Title

Quantitative coherent anti-Stokes Raman scattering (CARS) microscopy of skin optical clearing dynamics

Authors

Zimmerley, Max
Choi, Bernard
Potma, Eric O

Publication Date

2008

DOI

10.1364/biomed.2008.bwd7

Quantitative coherent anti-Stokes Raman scattering (CARS) microscopy of skin optical clearing dynamics

Max Zimmerley[*], Bernard Choi[‡] and Eric O. Potma[‡*]
Department of Chemistry & Beckman Laser Insitute ‡, University of California, Irvine*
epotma@uci.edu

Abstract: CARS microscopy is used to quantitatively investigate the process of skin optical clearing. Using glycerol and dimethyl-sulfoxide as the clearing agents, we find that tissue scattering is a highly nonlinear function of agent concentration.

OCIS codes: (180.4315) Nonlinear microscopy; (170.3880) Medical and biological imaging; (170.7050) Turbid media.

1. Introduction

Nonlinear coherent imaging techniques such as second harmonic generation (SHG) microscopy and coherent anti-Stokes Raman scattering (CARS) microscopy have come increasingly more in vogue as visualization tools in biological imaging studies. These nonlinear techniques not only offer noninvasive, submicron resolution imaging of cellular samples and bio-tissues, they also provide a series of valuable intrinsic contrast markers. SHG microscopy has rapidly gained popularity because of its high sensitivity to fibrillar protein structures such as collagen.[1, 2] CARS microscopy, on the other hand, boasts molecular specificity through its vibrational sensitivity.[3, 4] Lipid, water and protein structures have been selectively visualized with the CARS imaging microscope, adding a rich collection of molecular markers to the biological microscopist's probe arsenal. Multimodal combinations of these contrast mechanisms have been used in nonlinear imaging studies of nerve tissue[5] and tumor tissue[6].

Despite their useful contrast of biological relevance, SHG and CARS signals are difficult to interpret quantitatively. Both techniques produce coherent radiation that is not only quadratic in molecular concentration, it is also characterized by changing portions of forward and backward scattered signal across the sample.[7] The emission profiles result from interference of the coherent signal waves, as dictated by the size, shape and orientation of tissue structures in focus. After generation, the coherent radiation is scattered by the tissue, which further affects the amount of signal observed in each detection direction. These effects complicate a quantitative assessment of the acquired SHG and CARS images. Most SHG and CARS studies so far have focused predominantly on qualitative features in the images. It is clear that with a more quantitative approach, the applicability of both techniques would be increased significantly.

In this contribution we employ multimodal SHG/CARS imaging for a quantitative examination of the process of skin optical clearing. It is shown that by collecting forward and backward coherent signals simultaneously, meaningful biophysical parameters can be attained. This approach reveals a clear and quantitative picture of the elusive skin clearing process.

2. Skin optical clearing

Several chemical compounds, such as glycerol and dimethyl sulfoxide (DMSO), induce a temporary transparency of the skin when applied topically. Skin transparency significantly facilitates optical investigations at greater depths into the tissue, and aids visualization of tissue structures typically blurred by the opacity of dermal and epidermal layers.[8] Nonetheless, the biophysical origin of the optical clearing phenomenon is currently under debate. One interpretation asserts that replacement of tissue water by a higher refractive index solvent leads to an improved refractive index matching between native tissue components and their immediate surroundings.[8] Such a model suggests that tissue transparency is the direct result of reduced scattering due to refractive index matching. Another model hypothesizes that skin-clearing chemicals temporarily dissolve the highly organized fibrillar collagen network in the dermal layer.[9] In this view, the reduced Mie-scattering of the collagen matrix would directly improve tissue transparency. The collagen solubility model is fuelled by recent *in vitro* experiments on collagen gels, which confirmed that glycerol disassembles collagen fibers and lowers tissue scattering.[9]

One of the difficulties in unraveling the mechanism of optical skin clearing is that the local, time-varying concentration of skin-clearing agent is typically inaccessible in conjunction with the changing tissue scattering coefficient and collagen distribution. Here we have combined the SHG and CARS modalities, together with

transmission imaging, to simultaneously probe agent concentration, tissue transmission and collagen density during the dynamic process of optical clearing in human skin.

3. Quantitative multimodal imaging

We have constructed a multimodal microscope interfaced with a picosecond laser system, which delivers a tunable pulse train in the 760 - 960 nm range along with a fixed pulse train at 1064 nm. Our beam-scanning microscope is equipped with three detectors. Two forward detectors monitor the transmission of the incident laser light and either the SHG or CARS signal. A third detector captures the SHG/CARS signal in the epi-direction. All detectors are configured in the non-descanned mode in close proximity to the objective lens for maximum signal collection. In addition, our microscope is outfitted with a confocal Raman spectrometer for acquisition of Raman spectra from selected spots in the focal imaging plane.

Transparency measurements were done on excised human skin. Skin samples were cut to a thickness of about 0.5 mm and mounted between cover slips. Clearing agents where applied topically from the dermal side, stratum corneum side or sideways onto the full cross sectional face of the tissue slab. During the clearing agent diffusion process through the tissue, CARS/SGH and transmission images were taken every 15 seconds over a period of several hours.

We first investigated the effect of clearing agents on the collagen network. Figure 1 shows E-SHG images of typical collagen patterns 40 minutes after application of glycerol or DMSO. Clearly, both agents alter the bundle structure of collagen fibers. Glycerol disrupts the smooth bundle structure into fiber networks that appear significantly more ruffled. DMSO, on the other hand, reorganized the linear strokes into a more knotted distribution while maintaining bundle smoothness. At all times, no major reduction of the fiber concentration was observed with either one the clearing agents, casting some doubt on the collagen solubility model.

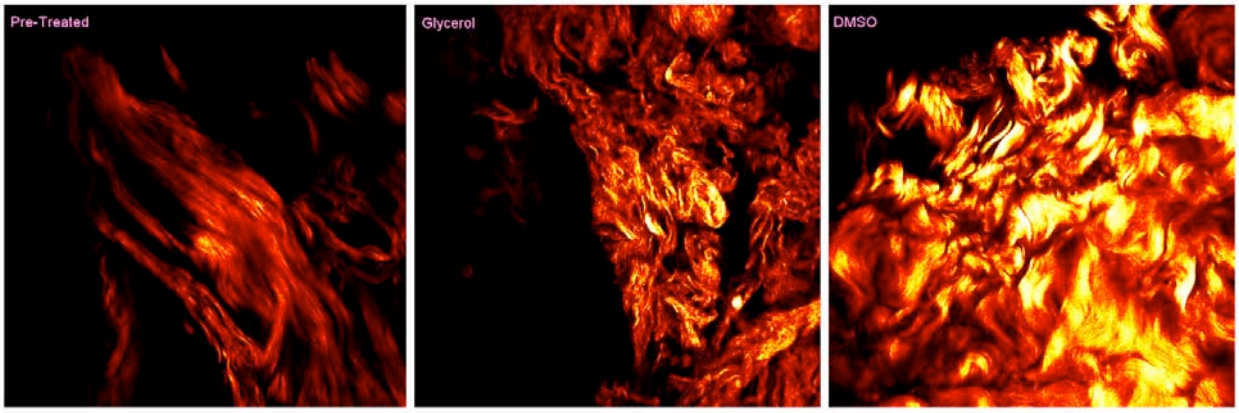

Fig. 1. SHG images revealing the typical collagen patterns observed before treatment (left panel) and after treatment with glycerol (middle panel) or DMSO (right panel). Images are 150 x 150 μm. Image acquisition time is 1.5 seconds/frame.

The power of the multimodal imaging approach is that the qualitatively changing collagen patterns can be correlated with the clearing agent concentration and the optical attenuation of the sample. Figure 2 shows the CARS spectrum of DMSO in the CH stretching region. The CH_3 symmetric stretch at 2913 cm^{-1} is an ideal target band for visualizing the diffusion of DMSO through the tissue using CARS microscopy.

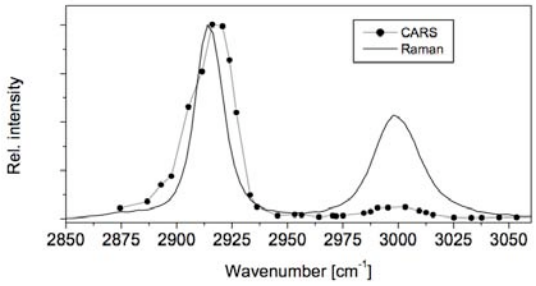

Fig 2. Raman and CARS spectrum of optical clearing agent DMSO.

Figure 3a depicts the time-varying CARS signal from DMSO, along with the tissue transmittance, immediately after application of the agent from the side, imaged 50 μm into the dermis (sample oriented with beam coming in

from dermal side). As expected, the tissue transmittance increases over time. In addition, several interesting features are observed. First, during the first few minutes, the transmittance increases much faster than forward CARS (F-CARS) signal. This indicates that the changing scattering properties of the tissue do not linearly scale with the DMSO concentration. Second, while the F-CARS signal rises at all times, the epi-CARS signal (E-CARS) first dips and rises only after ~10 minutes. This effect is explained by the fact that the majority of E-CARS signal results from back-scattering of forward propagating CARS radiation. Increased transmission implies reduced scattering and hence less E-CARS signal. The higher DMSO concentrations are reflected in the E-CARS channel only after the initial loss in scattering is balanced out by the stronger forward propagating CARS levels.

This example shows that a single channel detection of the CARS signal is insufficient to quantitatively determine the DMSO concentrations in a scattering tissue. By carefully analyzing both the forward and backward CARS signals in conjunction with the tissue transmittance, we can correlate the local DMSO concentration to tissue scattering. Using the F/B ratios, which are independent of concentration, we are able to determine the changing tissue attenuation coefficient *g* at the CARS wavelength, defined by:

$$S_{CARS} \propto S^{0}_{CARS} \cdot e^{-gL}$$

where L is the thickness of the tissue and S^{0}_{CARS} is the total CARS signal generated at the focal volume. The tissue attenuation constant $g(t)$, shown in Figure 3b, accurately reflects the time dependent scattering characteristics of the tissue. Once $g(t)$ is known, the DMSO concentration can be obtained from scattering-free concentration calibration curves. The result is that actual concentration levels can be quantitatively correlated to tissue scattering. Interestingly, as we have seen, tissue scattering is a highly nonlinear function of clearing agent concentration. Such correlations provide important clues as to the nature of the optical clearing effect. Using this recipe, we have also been able to correlate DMSO or glycerol concentration levels to morphological changes to the collagen network.

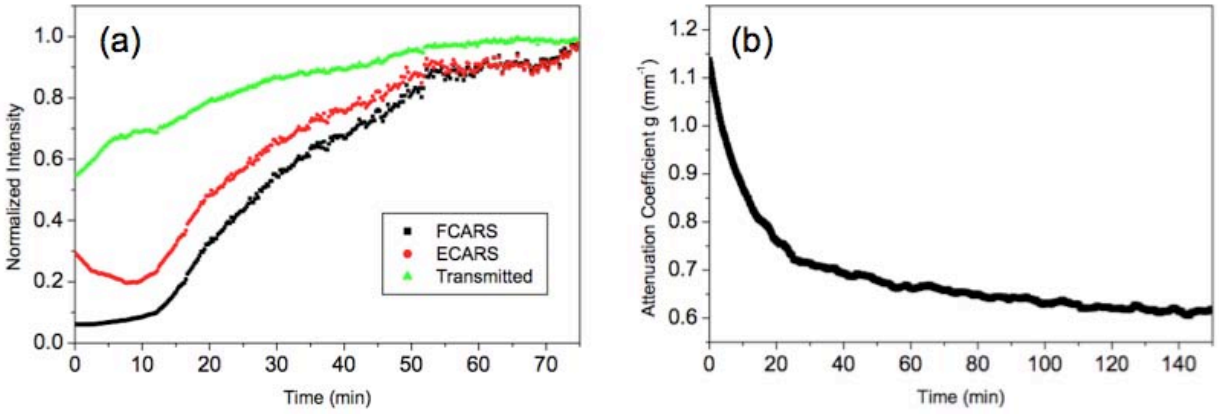

Fig.3. Dynamic recording of skin optical clearing process. (a) Time dependent CARS and transmission signals of human skin after application of DMSO. (b) Extracted attenuation coefficient g(t), showing the reduced scattering of the tissue due to the increasing DMSO concentration.

4. References

1. P. J. Campagnola and L. M. Loew, "Second-harmonic imaging microscopy for visualizing biomolecular arrays in cells, tissues and organisms," Nat. Biotechnol. **21**, 1356-1360 (2003).
2. W. R. Zipfel, R. M. Williams, R. Christie, A. Y. Nikitin, B. T. Hyman, and W. W. Webb, "Live tissue intrinsic emission microscopy using multiphoton-excited native fluorescence and sceond harmonic generation," Proc. Natl. Acad. Sci. USA **100**, 7075-7080 (2003).
3. J. X. Cheng, "Coherent anti-Stokes Raman scattering Microscopy," Appl. Spectrosc. **91**, 197-208 (2007).
4. J. X. Cheng and X. S. Xie, "Coherent anti-Stokes Raman scattering microscopy: instrumentation, theory and applications," J. Phys. Chem. B **108**, 827-840 (2004).
5. T. B. Huff and J. X. Cheng, "In vivo coherent anti-Stokes Raman scattering imaging of sciatic nerve tissues," J. Microsc. **225**, 175-182 (2007).
6. T. T. Le, C. W. Rehrer, T. B. Huff, M. B. Nichols, I. G. Camarillo, and J. X. Cheng, "Nonlinear optical imaging to evaluate the impact of obesity on mammary gland and tumor stroma," Mol. Imag. **6**, 205-211 (2007).
7. J.-X. Cheng, A. Volkmer, and X. S. Xie, "Theoretical and experimental characterization of coherent anti-Stokes Raman scattering microscopy," J. Opt. Soc. Am. B **19**, 1363-1375 (2002).
8. V. V. Tuchin, "Optical clearing of tissues and blood using the immersion method," J. Phys. D **38**, 2497-2518 (2005).
9. J. Hirshburg, B. Choi, J. S. Nelson, and A. Y. Yeh, "Collagen solubility correlates with skin optical clearing," J. Biomed. Opt. **11**, 040501 (2006).